ANALYZING THE DMLS-PROCESS BY A MACROSCOPIC FE-MODEL

F. Niebling, A. Otto, M. Geiger

Chair of Manufacturing Technology, University Erlangen-Nuremberg, Germany

Abstract

The presented macroscopic FE-model allows to analyze the thermal fields and the resulting stress built up during Selective Laser Sintering. Process and material parameters are focused on Direct Metal Laser Sintering (DMLS). The FE-model is introduced and the assumptions for the model are given. Three different geometric models are discussed. The 3D-model shows the sintering of a single line, whereas 2D-models are used for longitudinal and crosscuts of the sintering process. Aim of the investigation is a more basic knowledge about the process, which will lead to a stabilization and optimization of the process.

Introduction

Selective Laser Sintering (SLS) is an additive Rapid Prototyping technology [1]. A 3D-computer model is sliced into layers and the layer information is transferred to a SLS-machine. This machine transmits the adequate layer information onto a powder bed, whereby the topmost layer is locally sintered, coherent to the sintered layers beyond. By reiteratively adding new powder on top and locally sintering with the energy of a laser beam a 3D part can be built. This technology was originally developed for making plastic prototypes at the University of Texas, Austin in 1987 [2]. The SLS-technology is today used for making plastic, metal and ceramic prototypes.

Metal SLS-prototypes can be produced by two different ways [3], the Indirect Metal Laser Sintering process (IMLS), developed by DTM and the Direct Metal Laser Sintering process (DMLS) of EOS [4, 5, 6]. Both processes use a binder and a structure component in the powders and the relatively to the structure component low melting binder component is molten by the energy of the laser beam.

The ILMS process by DTM uses polymer binders, which are burned out in following oven processes and the porous material is infiltrated with metal.

The DMLS process of EOS uses a powder mixture, consisting of metals with different melting points. Several powder mixtures are available from EOS. The bronze based powders can be processes in air whereas the steel based powders need an inert gas atmosphere during processing.

The presented FE-model is based on parameters of the DMLS process and for an easier experimental accessibility for the described investigations the bronze based powder Direct Metal 50-V2 [7] was chosen, but in principle it is possible to adapt the model to every variant of the SLS process.

Modeling the sintering behavior

As a simulation tool for the FE-model Sysweld [8] from ESI was used. It allows the implementation of so called phases with different temperature dependent material properties and a time and temperature dependent function can be implemented for a phase change. These features were used for the simulation of the SLS-process: One phase was assigned to the material

parameter of the powder and another phase was assigned to the material parameters of the sintered material. Furthermore, a function was implemented for the transformation from powder to sintered material. It converts the powder phase at the melting point of the binder (850 °C for Direct Metal 50-V2) to sintered material. Material properties of both phases meet at the melting point of the binder phase and have at this temperature properties of the molten material.

For the simulation of the thermal field, density and heat conductivity were measured at room temperature for powder and sintered material. Especially the heat conductivity depends strongly on the temperature and it differs by a factor of 60 for powder and sintered material at room temperature. For the powder, the laws derived by [9] were used to model the heat dependency. The temperature dependency of the sintered material was approximated by applying the same gradient as of a similar bronze. The specific enthalpy was derived from the specific heat capacity and the latent heat of the melting reaction of the fractions of the powder, weighted by their ratio.

The simulation of the thermomechanical reactions of the SLS-process requires in addition to the parameters above the temperature dependent material parameters for yield strength, elasticity modulus and expansion coefficient. These were measured for the sintered material. Yield strength for powder is set to 10 MPa, because a lower yield strength caused instabilities in the numerical calculations.

Finally, the heat coupling between laser beam and powder bed were modeled. A surface distributed energy coupling is not appropriate for metallic powder, as described in [10], so an approach similar to [11] with a volumetric heat source was used, **fig. 1**. The diameter of the heat source corresponds to the gaussian beam diameter at the interaction zone and was set to 400 μm. The depth of the heat interaction zone equals the average grain size and was set to 50 μm. The verification of the model is given in [12]. The approach is in good consistency with the experimental studies.
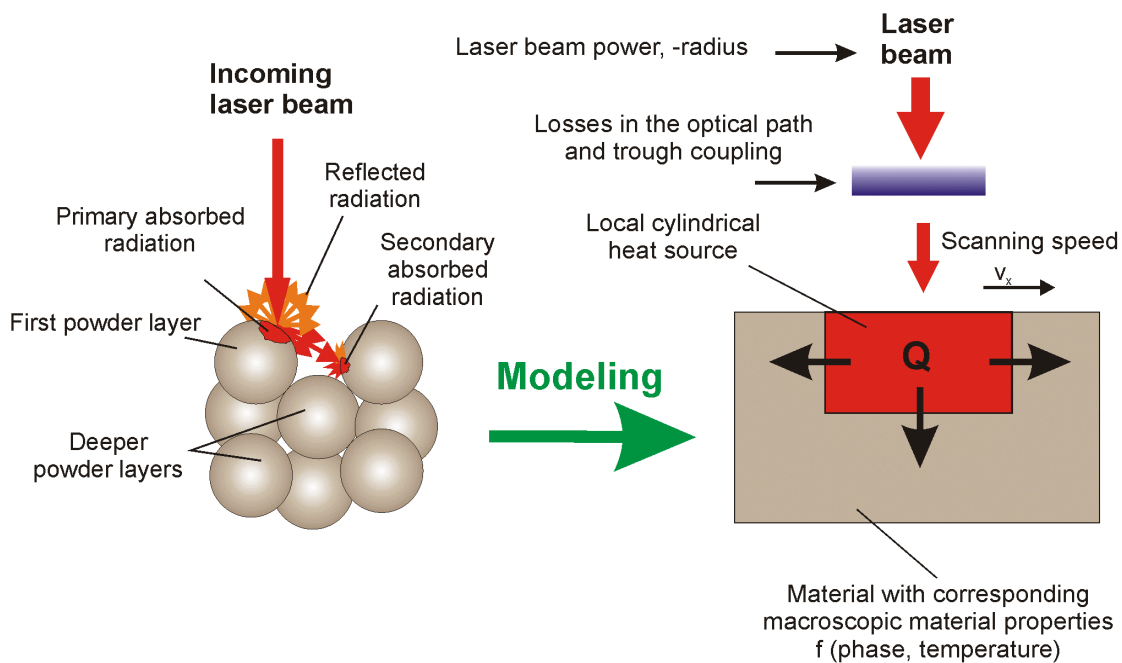
Fig. 1: *Model of the energy coupling of the laser beam into the powder bed*

Layer processing via SLS and derived geometric models for the FE-simulation

The top layer with the thickness h is locally exposed during the SLS-process to the energy of the laser beam corresponding to the layer information from the sliced computer model. The principle of layer exposition can be divided into two processing steps, **fig. 2**.

1. Processing of the contour   **2. Processing of the inner regions**

Laser beam

Basic material   Sintered material

z
x   y

h
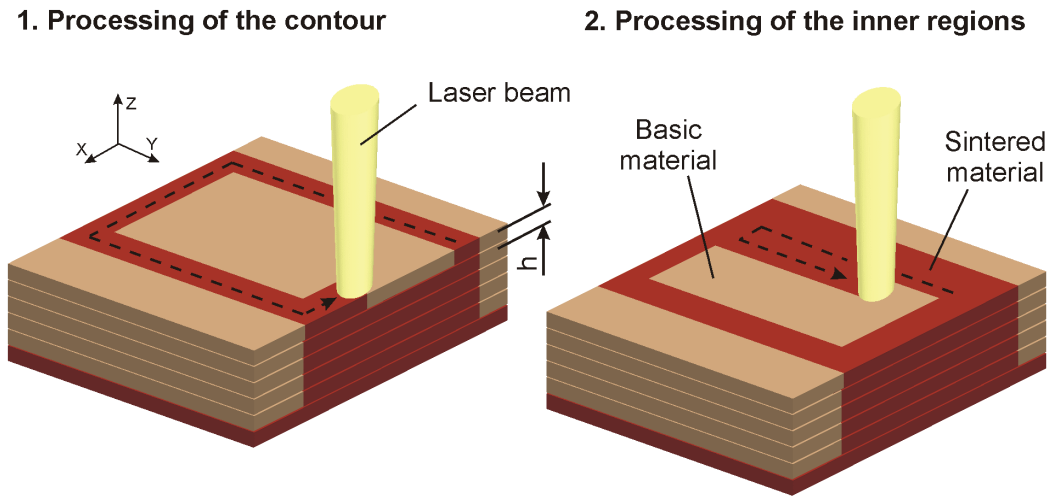
FE-models:

3D-model: Sintering of a line   2D-model plane strain: 2D-model plane strain:
- temperature development   longitudinal cut   crosscut
- stress built up   - temperature development
                                                               - stress built up
                                                                  during layer processing

Figure 2: Principle of laser exposition in the SLS-process

First, the contour is sintered with the energy of the laser beam which will form the side surface of the part. The process parameters of this line set important properties for the final part like e.g. the roughness. A main process parameter is the line energy E_L given by:

$$E_L = \frac{P_L}{v_S} \ ,$$

where P_L is the laser power and v_S is the scan speed. The line energy is responsible for the amount of locally molten material and sets the local cooling behavior as described in [12].

Secondly, the inner regions of the part are sintered by successive scanning over the powder bed. Besides the line energy, the area energy E_F has a main influence on the final part quality. The area energy is given by:

$$E_F = \frac{P_L}{h_S \cdot v_S} \ .$$

The area energy is the line energy divided by the offset between the successive scans, called the hatching distance h_S. The influence of the area energy on the part quality can be deduced from investigations in [13].

The FE-simulation of the complete processing within a 3D-model doesn't make sense at the state of the art of the accessible computer power and software solutions. Therefore the process was investigated with different geometric models: The processing of the contour is examined by a 3D-model, which models the sintering of a single line. Basic conclusions can be drawn from this model about the thermal field and the stress built up. The complex process of filling the part by iterative scanning on the inner regions can be investigated by 2D-models of a longitudinal cut and a crosscut through the processed part. The mechanical model is simulated as plane strain to show up the theoretical maximum of stress generation within the processing.

Thermal and stress field for sintering lines

A 3D-model as shown in **fig. 3** was used to gain knowledge about the processing of the contour line and for acquiring basic information about the thermal and stress field during the sintering process. On a sintered stress free part with 4 mm length and a height of 1 mm a powder layer of 0,1 mm thickness is applied. The part has ambient temperature in it's initial condition. The sintering process starts by the laser beam activation and the laser is moved over the powder bed for a length of 3 mm. Because of symmetry conditions only one half of the part was modeled. 35552 nodes and 31500 elements were used in the spatial FE-model.
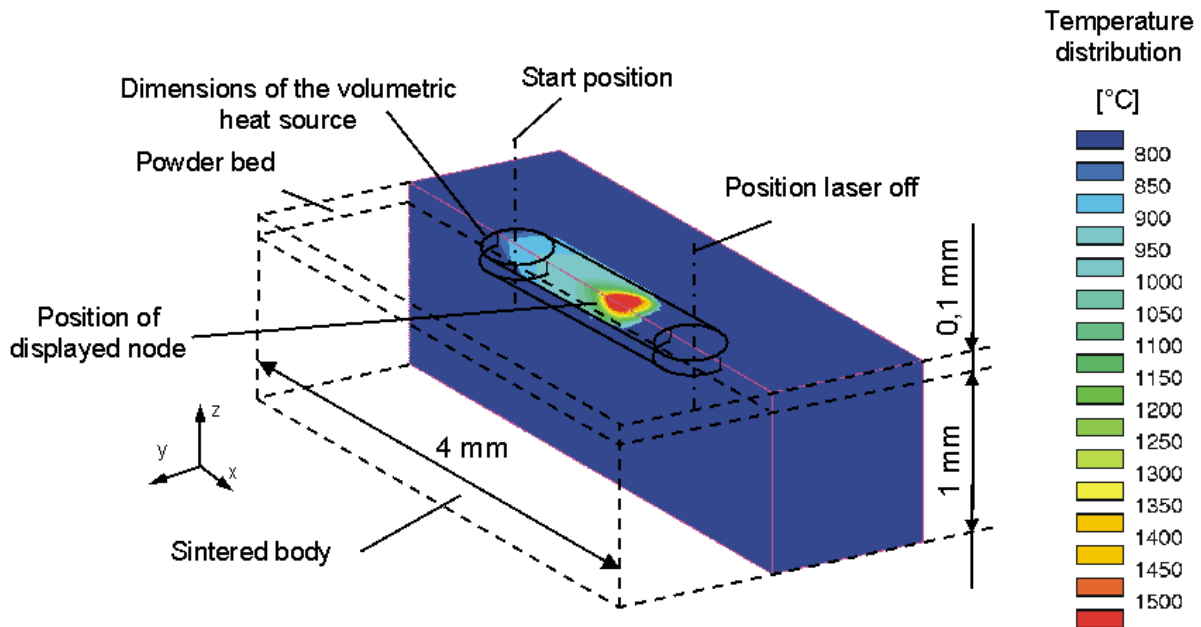
Figure 3: Temperature distribution embedded in geometric model for sintering a line

Fig. 4 shows the temperature and stress development for a node in the bottom of the powder layer on the symmetry plane, marked in **fig. 3**. In the region between the layers delamination as a process failure can occur. It is therefore especially interesting, to study the temperature and stress development in this region.

For a time span of about 3 ms the temperature locally exceeds 850 °C, the melting temperature of the binder material. The binder is molten and in the FE-model a phase change

from powder material to sintered material takes place in this region. Material properties are at these temperatures those of the molten material, visible e.g. in the decreased yield strength.
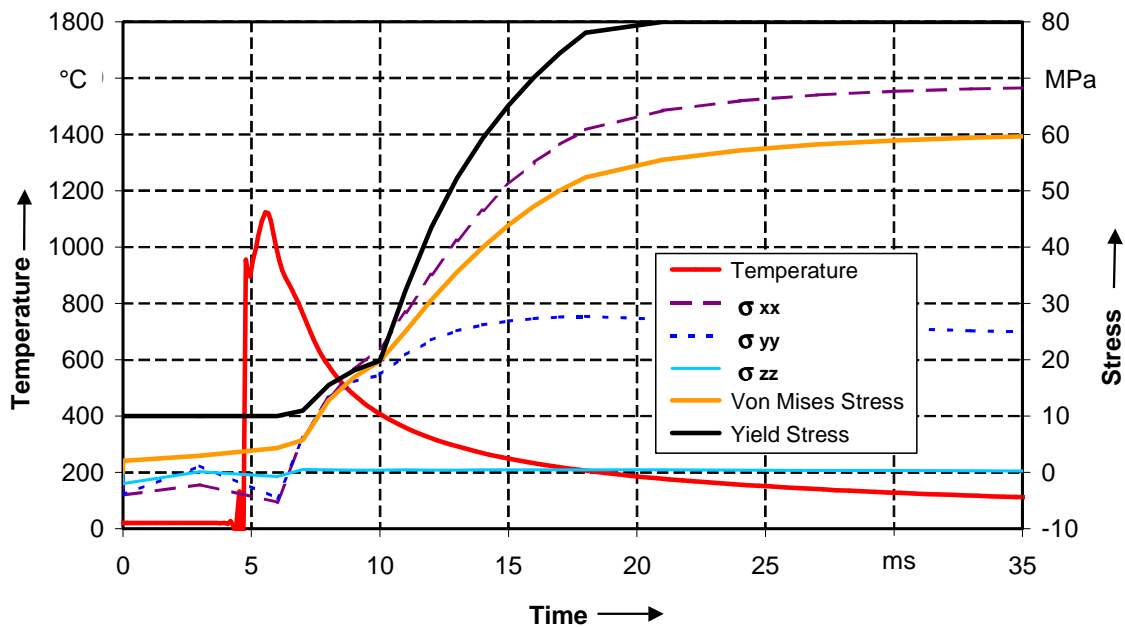
Figure 4: Temperature and stress development between the layers in the middle of a sintered trace. Process parameters: P_L: 151 W, v_S: 294 mm/s

In the following cooling tensile stresses increase, mainly in the longitudinal direction to the sintered trace, caused by strain obstruction of the contracting sintered trace. The von Mises stress builds up and reaches asymptotically a constant value of about 60 MPa. The resulting internal stresses can cause warpage of the part, if heated successively. Furthermore, in the early local cooling stage, the von Mises stress gains similar values like the yield stress and the elastic deformation ability of the material about 5 ms after solidification is nearly depleted. The buckling in the yield stress curve at 400 °C is due to a change in the tangent of the yield limit curve at these temperatures. The material behavior at temperatures beyond 400 °C is brittle which means that internal tensile stresses with a von Mises stress loading near to the yield limit can cause a crack initiation. The results of the simulation aim therefore to a possible origin of the delamination in the early local cooling.

Longitudinal cut through the building process: Influence of scan vector length on temperature development

Part properties as e.g. density depend on the scan vector length, [14]. The scan vector length influences therefore the local thermal field during the sintering process. The thermal field can be described locally by the maximum temperature and the successive cooling behavior.

The longitudinalcut FE-model was used to study this effect. The geometry of the model is shown in **fig. 5**. It has 12768 nodes and 12540 elements.
The model is described in detail in [12]. In the following only the result of the dependency of the maximum temperature on the scan vector length is shown.

388
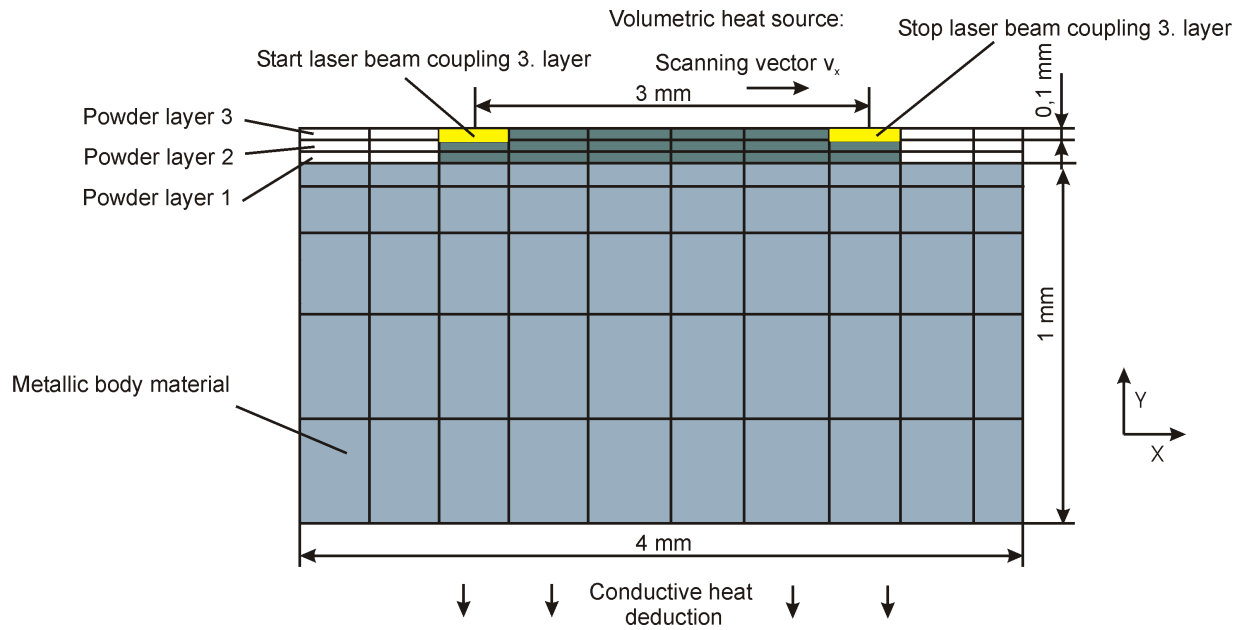
Fig. 5: Geometric model for the longitudinal cut through the sintering process. Shown number of elements is reduced.

The dependency of the maximum temperature on the scanning way was studied by a parameter variation. Scan speed and line energy were varied, **fig. 6**. The maximum temperature is attained at about the same scanned distance, independent of the scan speed and with a light dependency on the line energy. In the given example, at about 0,4 mm, which corresponds to the diameter of the laser beam on the powder bed. The temperature field is stabilized in the molten area at the interaction zone at that point. Therefore, it can be assumed that the dependency of material properties on the scan vector length is mainly due to a different local cooling behavior, caused by the different shape of the sintered upper layers. In the sintering process heat is dissipated mainly in the sintered body due to the strong differing heat conductivity of metal powder and sintered body.
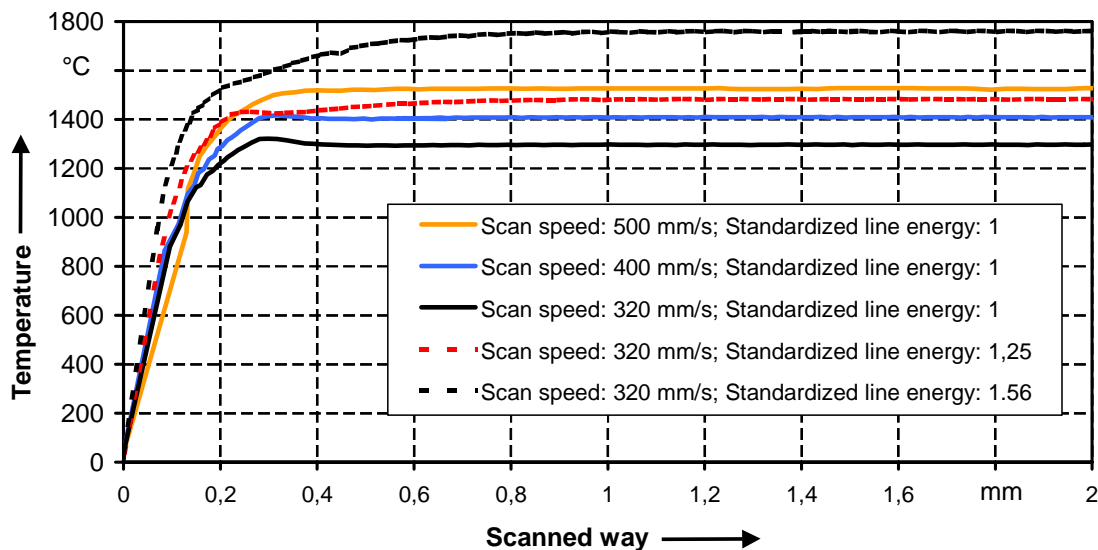
Fig. 6: Maximum temperature vs. scanned distance. Scan speed and line energy varied.

389

Crosscut trough the building process

Geometric measures of the crosscut model are shown in **fig. 7**. This model is used for studying the effects of scanning strategies on the thermal field during processing and the resulting stress field. The geometric model has 3752 nodes and 3630 elements.
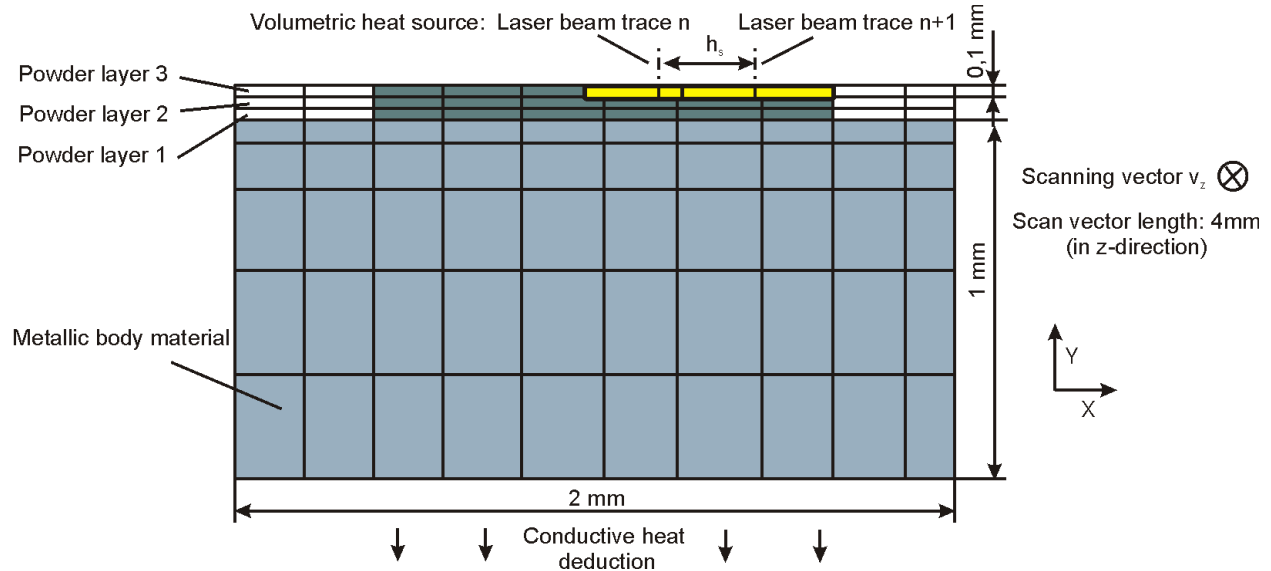
Fig. 7: Geometric model for the crosscut through the sintering process. (Shown number of elements is reduced.)

In **fig. 8**, the von Mises stress distribution of a cooled part, sintered on a platform as a result of different scanning strategies is shown. Both scanning strategies were simulated with the same resulting area energy E_F. Within the left scanning strategy, the stress distribution in the part is textured and the high stress loaded regions are at the edges. Together with the notch effect of the side shape results a critical processing leading to a high possibility for delamination. The example on the right side displays the result with a changed scanning strategy. The stress field is more uniform and areas of highest internal stresses are not near to the edges anymore.
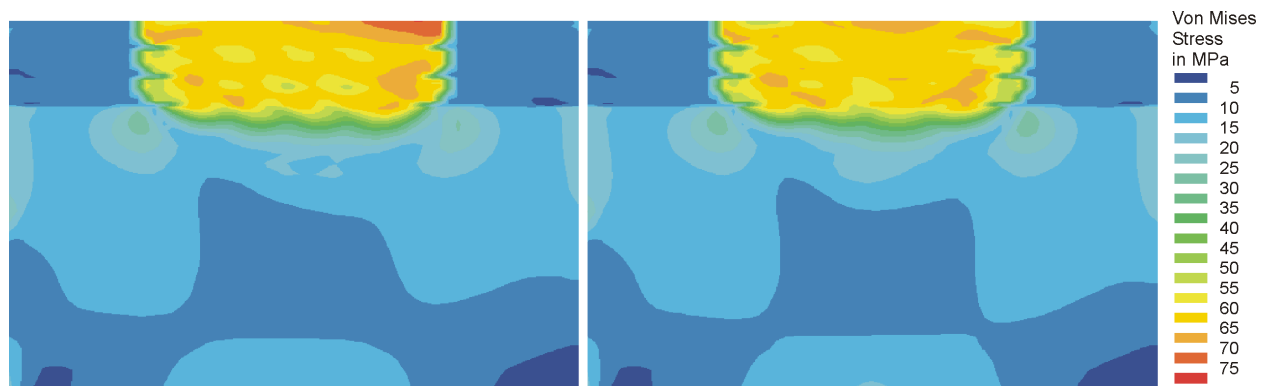
Fig. 8: Resulting von Mises stress distribution of a sintered part on a platform for different scanning strategies. E_F was kept constant.

390

Summary

A macroscopic FE-model is presented, which is capable of analyzing the transient temperature and stress field of the DMLS process. The model describes the powder and the sintered body with temperature dependent material properties and the process of local powder melting and cooling in a sintered condition. Results of a 3D-model of sintering a line indicate, that a possible crack initiation, which results in the process failure delamination is initiated in the early local cooling stage. Results of the 2D longitudinal cut FE-model indicate, that geometric size dependent effects like different porosity for identical machining parameters are due to changes in the cooling behavior. A significant change of the maximum temperature can not be observed for a scan length more than 0,4 mm, which means a stabilization of the heat input and output. Within a 2D-cross section model the influence on the stress development of scanning strategies can be studied. The macroscopic FE-model therefore gives basic predictions for a stabilization and optimization of the DMLS process.

Acknowledgement

References

[1]   Burns, M.: Automated fabrication: Improving productivity in manufacturing. Los Angeles: Ennex Corporation (1993)

[2]   Deckard, C. R.; Beaman, J.J.: Recent advances in selective laser sintering. In: Proc. of the 14th Conf. on Production Research and Technology. Michigan, USA, 1987, p. 447-451

[3]   Wholers, T.: Wohlers Report 2000 - Rapid Prototyping & Tooling State of the Industry. Annual Worldwide Progress Report. Wohlers Associates, Inc., Fort Collins, Colorado, USA (2000)

[4]   Nyrhila, O.; et al.: Industrial Use of Direct Metal Laser Sintering, In: 9. SFF Symposium (1998), Austin, Texas, 487-493

[5]   Petzoldt, F.; et al.: Functional Components and Molds Produced by Lasersintering. In: International Conf. on Powder Metallurgy and Particular Materials, Chicago, USA (1997), 21ff.

[6]   Geiger, M; Coremanns, A.: Lasergestütztes Rapid Tooling – Vorserienwerkzeuge zur Herstellung funktionsfähiger Bauteile mit Endprodukteigenschaften. In: Wege kennen – Potentiale nutzen. 6. Umformtechnisches Kolloquium, Darmstadt (11.-12. 3. 1997), p. 175-193

[7]   Datenblatt Direct Metal 50 V2. EOS GmbH, München

[8]   Sysworld `99: Technical Description of Capabilities, ESI Group (1999), France

[9]   Sih, S.; Barlow, J.: The prediction of the thermal conductivity of powders. In: Proc of 6. SFF, Austin, Texas, 1995, p. 397-402

[10]   Wang, X. C.; Kruth, J. P.: A Simulation model for Direct Selective Laser Sintering of metal powders. , Leuven, Belgium, 2000, CIVIL-COMP Ltd., Edinburg, Scotland, p. 57-71

[11]   Sun, M; Beaman, J.: A Three Dimensional Model for Selective Laser Sintering. In Proc. of SFF, Austin, Texas 1991, p. 102-109

[12]   Niebling, F.; Otto, A.: FE-simulation of the Selective Laser Sintering Process of Metallic Powders. In: Geiger, M.; Otto, A.: LANE 3, Meisenbach Verlag, Bamberg, 2001, p. 371-382

[13]   Coremans, A.: Direktes Laserstrahlsintern von Metallpulver - Prozeßmodellierung, Systemtechnik, Eigenschaften laserstrahlgesinterter metallischer Werkstücke. Meisenbach Verlag, Bamberg,1999

[14]   Coremans, A.: Groot, D.: Residual stresses and thermal stability of laser beam sintered metal parts. In: Geiger, M.; Vollertsen, F.: LANE 2, Meisenbach Verlag, Bamberg, 1997, p. 577-588